Kovove Mater. 50 2012 97–105
DOI: 10.4149/km_2012_2_97

New methodology of testing phase transformations in structural steels in welding thermal cycle conditions

M. Łomozik*

Testing of Materials Weldability and Welded Constructions Department, Instytut Spawalnictwa (Institute of Welding), ul. Bł. Czesława 16-18, 44-100 Gliwice, Poland

Received 15 August 2011, received in revised form 12 September 2011, accepted 12 September 2011

Abstract

The paper presents differences in the character of the course of a thermal cycle in welding conditions compared with the cycle of a traditional heat treatment. The author elaborates the methodology of testing austenite phase transformations in steels affected by welding thermal cycles; the said methodology has been developed and put in practice at Instytut Spawalnictwa in Gliwice. The results of related tests are presented in the form of CCT diagrams for welding conditions for the following grades of structural steels applied in power engineering sector: X10CrMoVNb9-1 (P91), X10CrWMoVNb9-2 (P92), X12CrCoWVNb12-2-2 (VM12-SHC), 7CrMoVTiB10-10 (P24) and 10CrMo9-10 (P22).

K e y w o r d s: phase transformations, welding thermal cycle, simulation, constructional steels

1. Introduction

One of the basic characteristics of steels necessary to determine the weldability on the latter for a given joining technology is the critical temperature, i.e. that marking the beginning and end of phase transformation of austenite in solid state steels during heating and cooling.

The specific character of welding conditions accompanying the heating and cooling of an element being welded is responsible for significant differences in the course and character of a welding thermal cycle if compared with the cycle of a traditional heat treatment. The said differences are presented in Fig. 1.

If compared with the cycles of traditional heat treatment, welding thermal cycles are characterised by [2]:

– very high heating and cooling speeds in the heat affected zone (HAZ) – in case of arc-based welding methods the aforesaid speeds may reach as much as 400 °C s^{-1} near the fusion line,

– very short hold times at the maximum temperature (in practice, the reaching of the maximum temperature is immediately followed by the cooling phase),

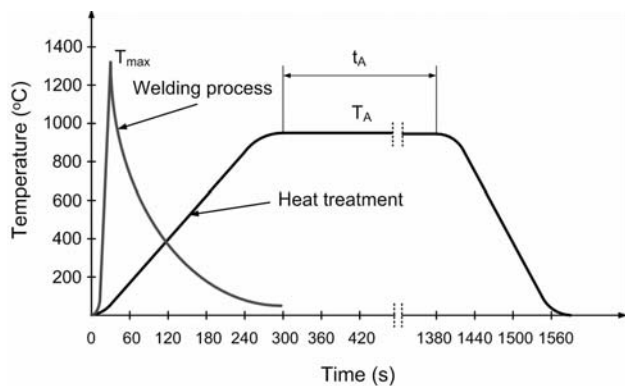

Fig. 1. Welding thermal cycle compared with traditional heat treatment cycle: T_A – austenitisation temperature, t_A – austenitisation time [1, 2].

– overlapping of two or more thermal cycles during multiple-pass welding.

Due to significant differences presented above, the values of critical temperatures of austenite phase transformations in steels are presented in diagrams of Continuous – Cooling – Transformation for welding conditions, i.e. *CCT for welding conditions* (*CCT-W*).

* Tel.: +48 32 3358 328; fax: +48 32 2314 652; e-mail address: Miroslaw.Lomozik@is.gliwice.pl

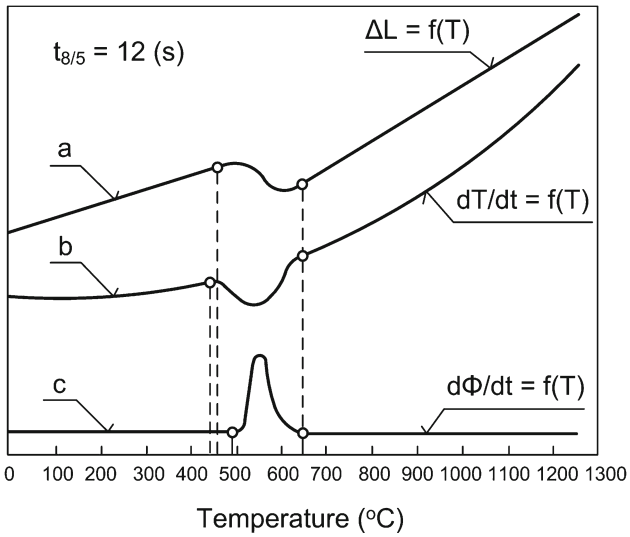

Fig. 2. Course of measurement curves during testing of phase transformations in steels and idea of determination of characteristic points: a) dilatometric curve, b) thermal analysis differential curve, c) magnetic flux curve as a function of temperature [3].

CCT-W diagrams constitute a source of essential information about the impact of welding thermal cycles on the structure and properties of steel being/to be welded and thus highly facilitate the development of welding technologies. At the moment, at various world's and Europe's research centres the values of critical temperatures of austenite transformations are determined using one measurement method only (usually the dilatometric method). In addition to that, at the aforesaid centres phase transformations in steels are tested in conditions characteristic of metallurgical conditions and not in welding ones.

2. Methodology of testing of phase transformations in steels in welding conditions

Material microstructures are formed depending on the parameters of a thermal cycle (maximum temperature and cooling speed). CCT-W diagrams can be developed as a result of the determination of critical temperatures of the beginning and end of individual phase transformations. In turn, the values of critical temperatures are determined on the basis of the measurement of three quantities characterising physical phenomena proceeding in steel under investigation, i.e. specimen dilatation, changes of magnetic properties and temperature in case of free cooling. The courses of individual variables, tested, in a function of temperature, with a phase transformations stand are presented in Fig. 2.

Methods for testing phase transformations in metallic materials were developed many years ago. In general, testing methods can be divided as follows:

a) *direct, i.e. "in situ" methods* – temperatures of phase transformations are determined during a welding process, using to this end the method of thermal analysis (usually by means of thermocouples);

b) *indirect (simulation) methods* – small-sized specimens are subjected to simulated welding thermal cycles, most faithfully reproducing heating and cooling phases as is the case during a real welding process.

Today, at Instytut Spawalnictwa in Gliwice, phase transformations in steels subjected to welding thermal cycles are tested by means of the simulation method, using a new test and measurement stand [3] presented in Fig. 3.

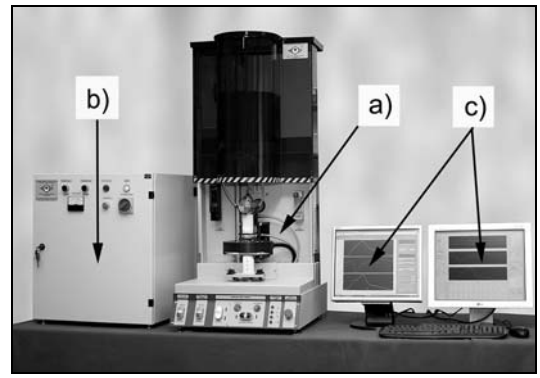

Fig. 3. Stand for testing phase transformations in steels in welding conditions (protective guard lifted): a) workspace with specimen being tested, b) supply and control system cabinet, c) monitors of control computer and computer for archiving measurement data.

The methodology of testing phase transformations is based on the simultaneous use of three measurement methods, i.e.:

– dilatometric method,
– magnetometric method,
– thermal analysis method.

Owing to the application of the aforesaid method, during related tests one may register three various quantities, i.e. specimen material dilatation, change of magnetic flux and temperature.

The newly developed test stand features a major novelty, i.e. a laser sensor allowing a touch-free measurement of specimen dilatation.

The shapes and dimensions of specimens subjected to tests are presented in Fig. 4.

An important issue embedded in tests of phase transformations in steels in welding conditions is the measurement of temperature. Due to the fact that in welding processes the changes of temperature in steel being tested are significant, temperature measurement should be characterised by appropriately high dynamics. For this reason, the optimum solution in the case under discussion is the measurement of temperature

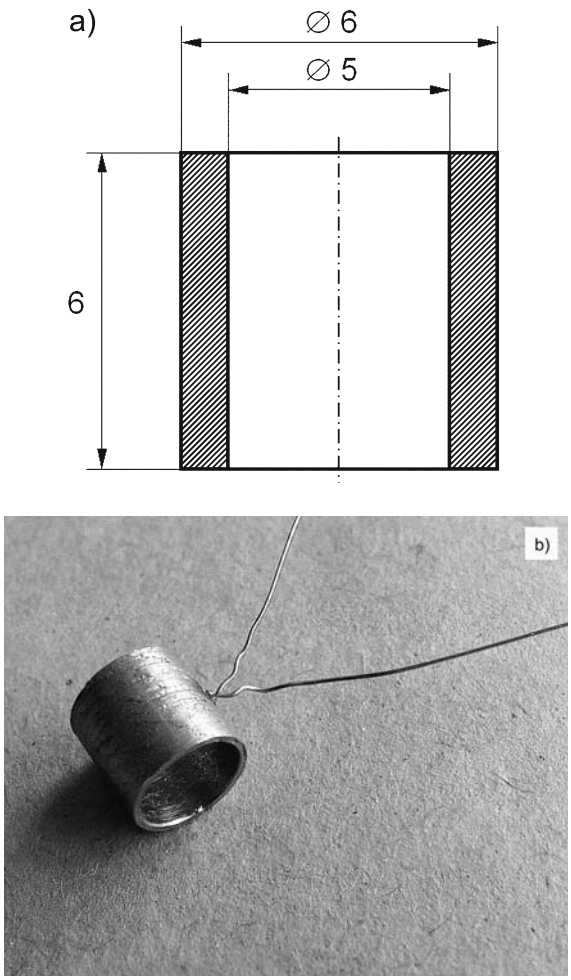

Fig. 4. Specimen used in tests of phase transformations: geometry and dimensions of specimen (a), specimen with K-type thermocouple (NiCr-Ni) welded to it (b).

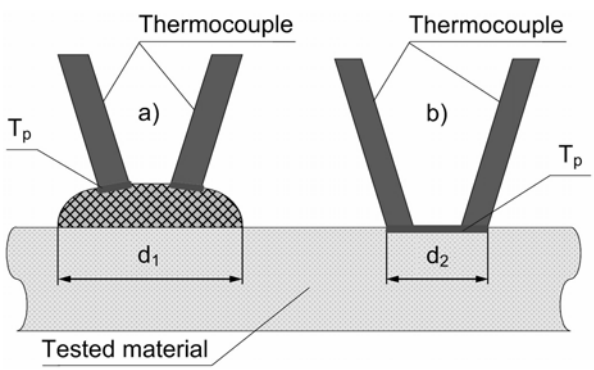

Fig. 5. Thermocouples: a) volumetric thermocouple with high volume of thermocouple joint and significant area of contact between joint and material in temperature measurement spot (diameter d_1), b) surface thermocouple with zero volume of thermocouple joint and smaller area of contact between joint and material in temperature measurement spot (diameter d_2).

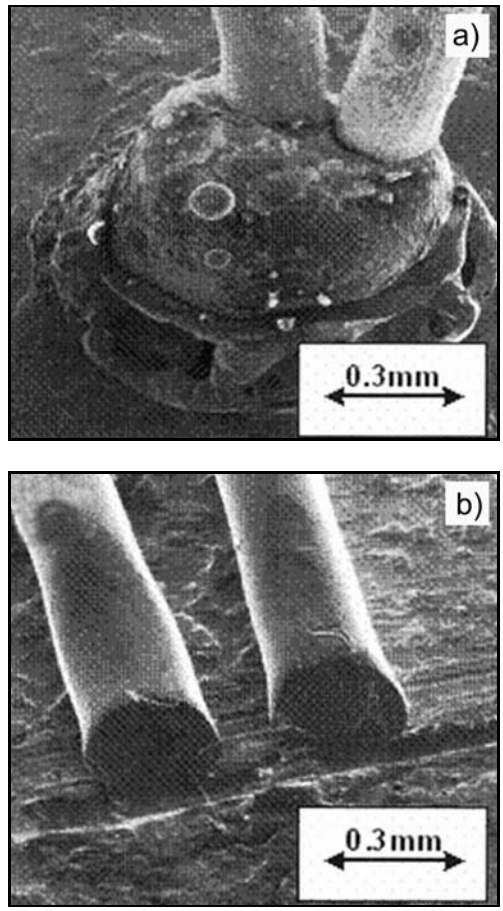

Fig. 6. Thermocouple joints: volumetric type (a), surface type (b), SEM photograph, mag. 100× [4].

with the use of thermocouples.

In the thermocouple-based method, the dynamics of temperature measurement varies and is predominantly dependent on the spot of temperature measurement, which, in turn, is conditioned by the type of a thermocouple joint [4] (designated in Fig. 5 with the symbol T_p). There are two types of thermocouple joints, i.e. volumetric and surface ones.

Figure 6 presents the main view of volumetric and surface thermocouple joints.

Higher dynamics of temperature measurement is characteristic of the surface type of joint (Figs. 5b, 6b), which is the consequence of its practically zero volume if compared with the volumetric type of joint (Figs. 5a, 6a). In addition to the foregoing, the temperature measurement spot (T_p) is located directly on the surface of a material being tested, e.g. steel.

In order to ensure the repeatability of the shape of surface-type thermocouple joints as well as to enable the positioning and production of joints in a precisely specified spot of the specimen under test, a specialised resistance micro-welder with an inverter controller was developed at Instytut Spawalnictwa. The aforesaid

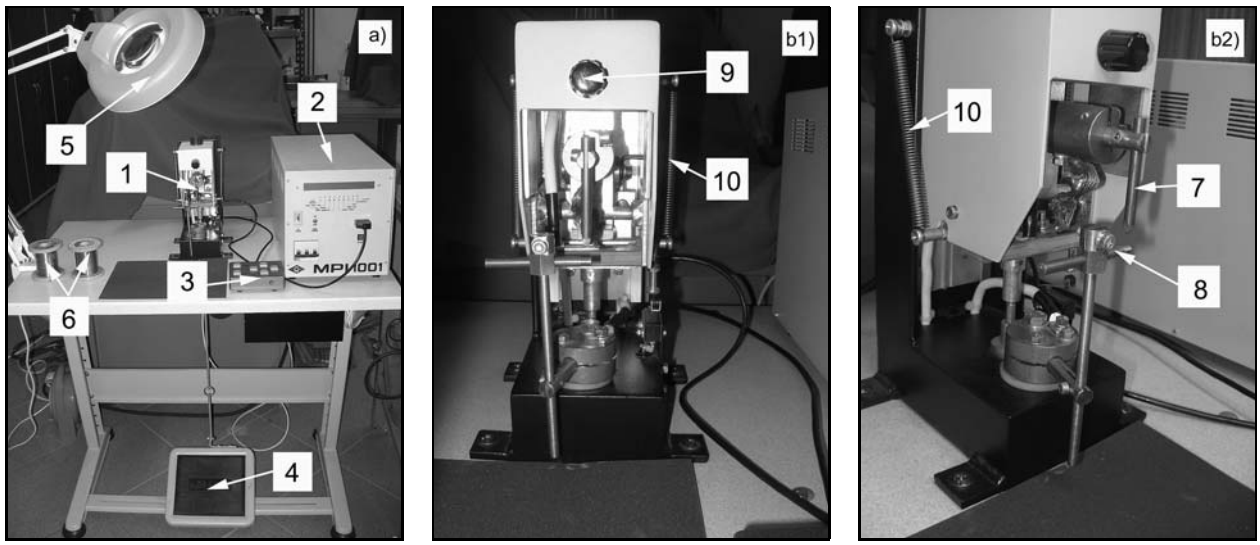

Fig. 7. Resistance micro-welder for welding of surface-type thermocouples to specimens: a) main view: 1 – system of micro-welder electrodes (head), 2 – inverter controller + power supply unit (inverter), 3 – control panel, 4 – pedal, 5 – magnifying glass to observe welding of thermocouple to specimen, 6 – thermocouple wires, b) micro-welder head: 7 – vertical electrode, 8 – horizontal electrode, 9 – electrode pressure force adjustment knob, 10 – electrode pressure system spring.

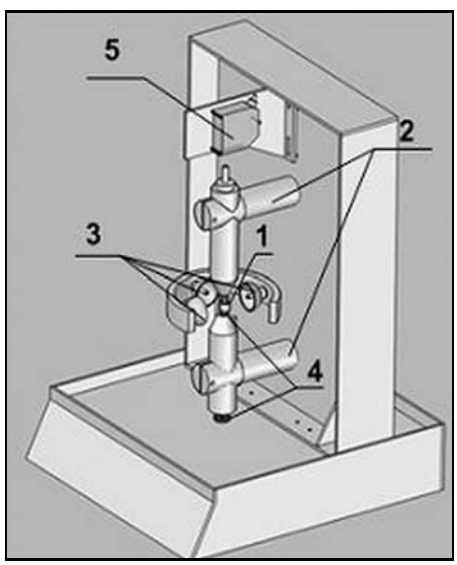

Fig. 8. Schematic presentation of main elements of working part of stand for testing phase transformations (explanation of designations – see text below).

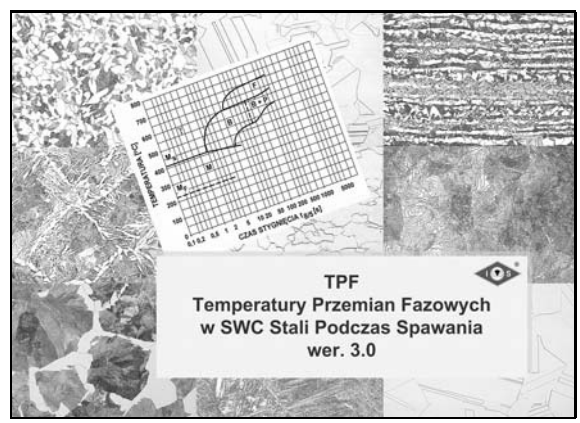

Fig. 9. Opening window of TPF ver. 3.0 programme for determining values of critical temperatures of phase transformations in steels and developing of CCT-W diagrams.

welding machine and its components are presented in Fig. 7.

Methodology of tests carried out with the test stand is as follows (Fig. 8):

– welding of thermocouple wires to the specimen under test with the use of the specialised micro-welder,

– placing the specimen being tested in the workspace of the measurement stand and connecting thermocouple wires to appropriate clamps,

– subjecting the specimen under test to simulated welding thermal cycles at the pre-defined value of cycle maximum temperature $T_{\max}$ and the value of cooling time $t_{8/5}$ (specimen cooling time within 800–500 ℃ temperature range),

– specimen under test (1), placed on thermally insulated base (quartz section) (4) and situated in the magnetic circuit of the yoke (2) with pole pieces is heated by the radiation of infrared heating lamps (3),

– thermal expansion of the specimen during a thermal cycle is registered by the laser sensor (5),

– measurement signals in the form of thermal, dilatometric and magnetic flux curves are registered in real time by the control and measurement equipment,

Table 1. Structural steels (under test) for operation at higher temperature

No.	Steel grade (steel symbol)	Microstructure of steel in initial state
1	X10CrMoVNb9-1 (P91)	tempered martensite
2	X10CrWMoVNb9-2 (P92)	tempered martensite
3	X12CrChoWVNb12-2-2 (VM12-SHC)	tempered martensite
4	7CrMoVTiB10-10 (P24)	bainite
5	10CrMo9-10 (P22)	ferrite + bainite

– transfer of measurement data from the PXI control computer (National Instruments-manufactured real-time processor) to the PC – archiving of data,

– processing and analysis of measurement curves, determination (on the curves) of characteristic points corresponding to the temperatures of the beginning and end of phase transformations in the steel being tested and automatic generation of a cumulative table with the values of critical temperatures using the TPF ver. 3.0 programme (Fig. 9),

– editing, correcting, approximating and recording of the curves on the CCT-W diagram in a separate working window of the TPF ver. 3.0 programme.

The testing procedure utilising the measurement stand makes it possible to carry out:

– tests involving three various measurement methods at the same time,

– three types of thermal cycles:

• *fast* – performed with cooling and shielding gas (in both cases argon) blown onto the specimen,

• *natural* – performed with free cooling of the specimen (only shielding gas flow switched on),

• *slow* – performed with reheating by means of the lamps during the specimen cooling phase (only shielding gas flow switched on),

– heating the specimen from ambient temperature to the maximum cycle temperature (approx. 1250 ℃), with the dynamics of between 6–14 s (presented values include also initial heating of infrared lamps – approx. 2 s),

– thermal cycles with cooling times $t_{8/5}$ from 2–1000s range.

3. Experimental materials, procedure and test results in the form of CCT-W diagrams

The range of structural steel grades for operation at higher temperature is presented in Table 1, whereas their chemical composition is presented in Table 2.

The steels under test were used to produce a series of specimens of the shape and dimensions as presented in Fig. 4. Afterwards, the specimens were subjected to simulated thermal cycles using the measurement stand described in the previous section. The shielding and cooling gas was argon representing technical purity. The maximum temperature of thermal cycles amounted to 1250 ℃, with the cooling times $t_{8/5}$ contained in the 2–600s range. Recording of the courses of individual thermal cycles for each combination of cycle parameters ($T_{\max}$, ℃, $t_{8/5}$, s) was followed by the archiving of primary measurement curves, i.e. those of temperature, magnetic flux and dilatation (thermal expansion). At the next stage, the programme TPF ver. 3.0 was used to determine the values of critical temperatures of individual phase transformations. The characteristic points on the measurement curves corresponding to the temperatures of the beginning and end of individual phase transformations proceeding in the steel being tested were determined by drawing tangents to the measurement curves and determining the point of deviation of the tangent from the measurement curve – Figs. 10–12.

Diagrams of austenite phase transformations in steels under test, in welding conditions CCT-W compared with CCT (*Continuous Cooling Transformation*) curves (diagrams for metallurgical conditions) are presented in Figs. 13–17.

4. Discussion

The comparison of CCT-W diagrams and CCT diagrams presented in Figs. 13–17 demonstrates a high similarity as regards the general character of the curves and the structural areas present on them. However, one can also observe clearly visible differences connected with the location of the curves in relation to the temperature axes. In general, in welding conditions, austenite phase transformations in steels in the solid state proceed in wider temperature ranges, i.e. they begin at higher and finish at lower temperatures if compared with metallurgical conditions. The above differences arise, first of all, from various values of steel austenitisation temperatures (higher for welding conditions), various austenitisation times t_A (for welding conditions time $t_A \ll 1$ s, whereas for metallurgical conditions time $t_A > 10$–15 min), various cooling times and cooling conditions of steels under test and various chemical compositions (within the same steel grade), for which both types of diagrams were developed.

T a b l e 2. Chemical composition of steels under test

Steel/composition	Chemical element content in %																
	C	Si	Mn	P	S	Cr	Ni	Mo	V	Ti	Nb	W	Co	Cu	B	Al	N
X10CrMoVNb9-1 (P91)	0.10	0.24	0.34	0.014	0.002	8.35	0.14	0.907	0.215	0.004	0.074	0.002	0.024	0.16	0.0002	0.012	0.066
X10CrMoVNb9-1 (P91) acc. [5]	0.08–0.12	0.2–0.5	0.3–0.6	max 0.02	max 0.01	8–9.5	0.4	0.85–1.05	0.18–0.25	–	0.06–0.1	–	–	–	–	0.040	0.03–0.07
X10CrWMoVNb9-2 (P92)	0.10	0.21	0.48	0.016	0.005	8.96	0.13	0.36	0.180	0.003	0.047	2.18	0.047	0.11	0.0022	0.018	0.0435
X10CrWMoVNb9-2 (P92) acc. [6]	0.07–0.13	0.5	0.3–0.6	max 0.02	max 0.01	8.5–9.5	0.4	0.3–0.6	0.15–0.25	–	0.04–0.09	1.5–2.0	–	–	0.001–0.006	0.04	0.03–0.07
X12CrCoWVNb12-2-2 (VM12-SHC)	0.12	0.46	0.28	0.026	0.004	11.99	0.25	0.18	0.250	0.006	0.038	1.69	1.54	0.08	0.0044	0.02	0.0465
X12CrCoWVNb12-2-2 (VM12-SHC) acc. [7]	0.1–0.14	0.4–0.6	0.15–0.45	0.02	0.01	11–12	0.1–0.4	0.2–0.4	0.2–0.3	0.005–0.018	0.03–0.08	1.3–1.7	1.4–1.8	0.25	0.003–0.006	0.02	0.03–0.07
7CrMoVTiB10-10 (P24)	0.10	0.36	0.58	0.009	0.002	2.30	0.18	1.051	0.262	0.081	0.0068	0.004	0.015	0.19	0.004	0.028	0.0082
7CrMoVTiB10-10 (P24) acc. [8]	0.05–0.10	0.15–0.45	0.30–0.70	0.02	0.01	2.2–2.6	–	0.9–1.1	0.2–0.3	0.05–0.1	–	–	–	–	0.002–0.007	0.02	0.01
10CrMo9-10 (P22)	0.11	0.22	0.45	0.007	0.003	2.02	0.09	0.96	0.007	0.003	0.0014	0.004	0.014	0.10	0.0002	0.018	0.0094
10CrMo9-10 (P22) acc. [5]	0.05–0.15	0.5	0.3–0.6	0.025	0.025	1.9–2.6	–	0.87–1.13	–	–	–	–	–	–	–	–	–

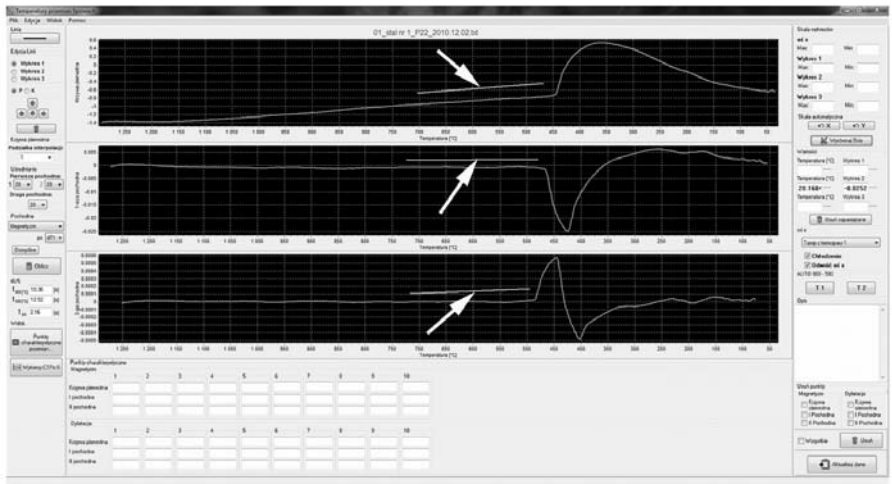

Fig. 10. Programme TPF. Manner of drawing tangents to measurement curves exemplified by magnetic flux curves.

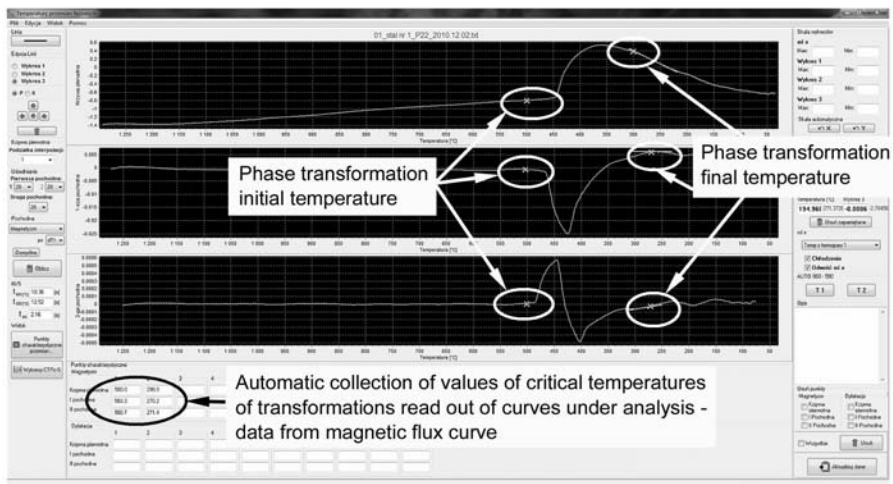

Fig. 11. Programme TPF. Determination of temperature of beginning and end of phase transformation on primary curve and 1-st and 2-nd derivative of magnetic flux.

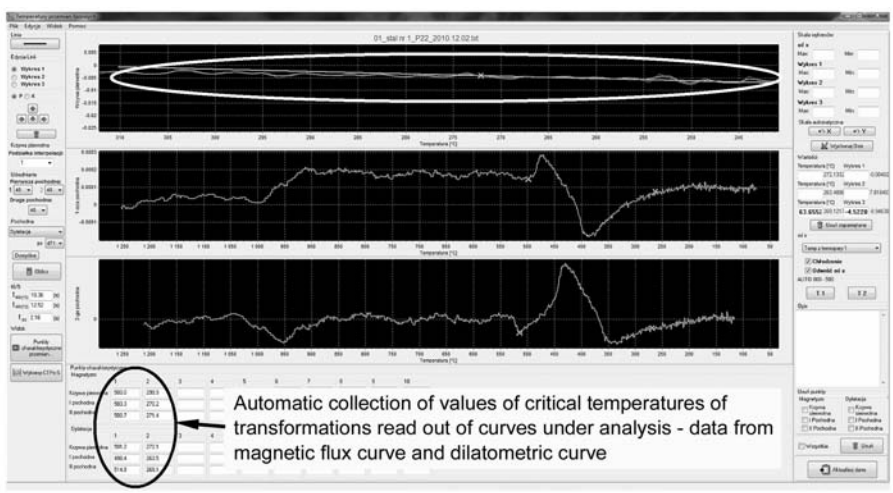

Fig. 12. Programme TPF. Possibility of enhancing accuracy of characteristic point reading by increasing fragment of measurement curve – example refers to analysis of dilatometric curve.

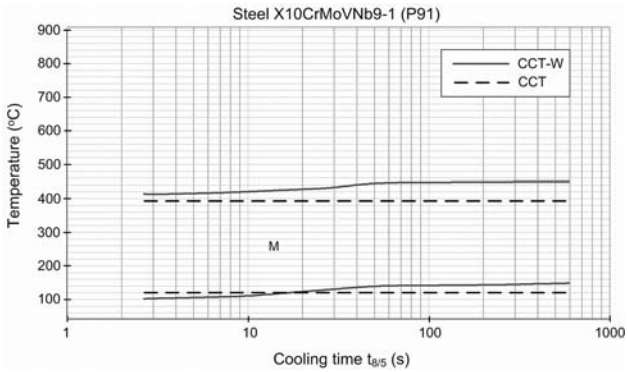

Fig. 13. CCT-W diagram compared with CCT diagram [9] for steel X10CrMoVNb9-1 (P91).

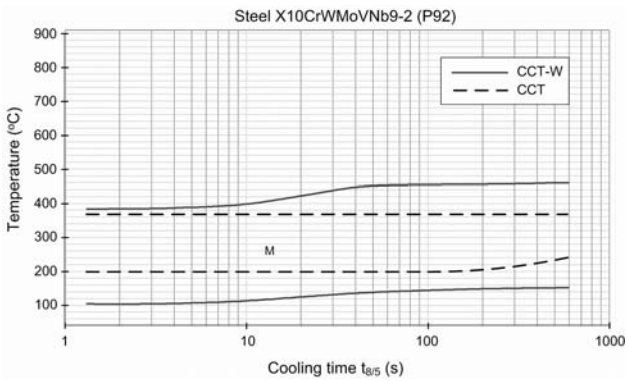

Fig. 14. CCT-W diagram compared with CCT diagram [9] for steel X10CrWMoVNb9-2 (P92).

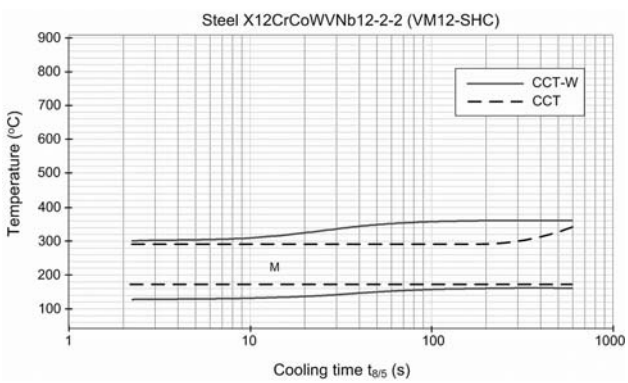

Fig. 15. CCT-W diagram compared with CCT diagram [9] for steel X12CrCoWVNb12-2-2 (VM12-SHC).

Structural steels applied in power engineering sector are usually alloy steels; their compositions being increasingly complex and containing significant amounts of chemical elements which, inter alia, strongly affect steel hardenability (e.g. chromium, molybdenum, boron, etc.), which, in consequence, is responsible for limited weldability of the aforesaid steels. For this reason, in order to avoid technological errors and limit the risk of crack occurrence in welded joints made of the said steels, designing of welded structures, development of welding technologies and the production of welded structures should draw on the knowledge revealed through phase transformations diagrams for welding conditions.

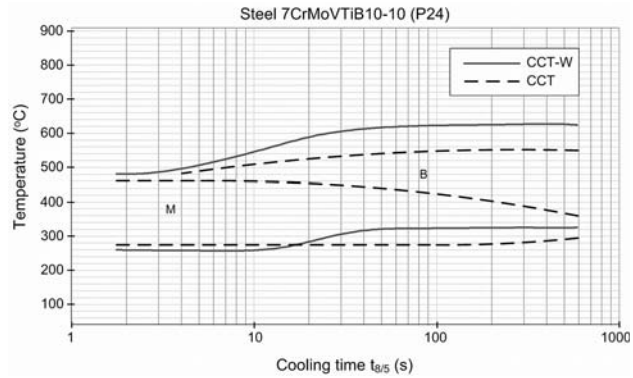

Fig. 16. CCT-W diagram compared with CCT diagram [10] for steel 7CrMoVTiB10-10 (P24).

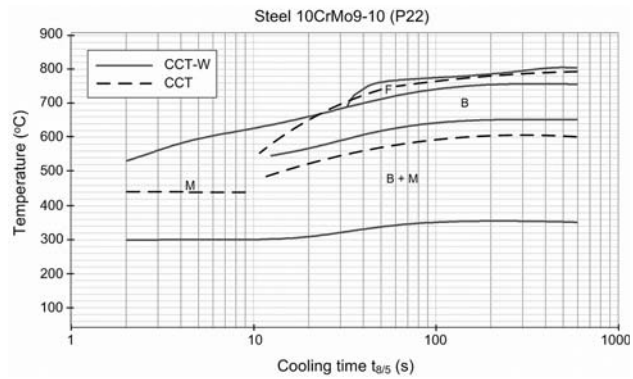

Fig. 17. CCT-W diagram compared with CCT diagram [11] for steel 10CrMo9-10 (P22).

5. Conclusions

1. In welding conditions, austenite phase transformations in steels in the solid state proceed in wider temperature ranges, i.e. they begin at higher and finish at lower temperatures when compared with metallurgical conditions.

2. Due to the aforementioned differences in the CCT-W diagrams and CCT diagrams it is recommended that while designing a welding technology and, in particular, determining pre-heating temperature and selecting post-weld heat treatment parameters one should use information resulting from welding diagrams (CCT-W).

Acknowledgements

This work was supported by the Ministry of Science and Higher Education of Poland under Instytut Spawalnictwa research project No. Id-137, 2010.

References

[1] PILARCZYK, J.—PILARCZYK, J.: Welding and Electric Surfacing of Metals. Katowice, Publishing House Śląsk Sp. z o.o. 1996.

[2] ŁOMOZIK, M.: Physical Metallurgy and Metallographic Tests of Welded Joints. Course Publication, Gliwice, Instytut Spawalnictwa 2005.

[3] MIKNO, Z.—GRZESIK, B.—ŁOMOZIK, M.—ZEMAN, M.—PILARCZYK, A.: Development of Measurement System and Methodology in Tests of Phase Transformations in Steels in Welding Thermal Conditions. Gliwice, Instytut Spawalnictwa, Research Project no. N505 002 31/0255, 2006–2009.

[4] SŁANIA, J.—MIKNO, Z.—WÓJCIK, M.: Welding Review, *12*, 2006, p. 23.

[5] PN-EN 10216-2:2009 Seamless Steel Pipes for Pressure Applications. Technical Conditions of Supply. Part 2. Unalloyed Steel and Alloy Steel Pipes with Specific Properties at Higher Temperature.

[6] RICHARDOT, D.—VAILLANT, J. C.—ARBAB, A. —BENDICK, W.: The T92/P92 Book, Vallourec & Mannesmann Tubes 2000.

[7] VdTÜV-Werkstoffblatt. Warmfester Stahl VM12-SHC. WB 560/2, 03.2009.

[8] ARNDT, J.—HAARMANN, K.—KOTTMANN, G. —VAILLANT, J. C.—BENDICK, W.—KUBLA, K.— ARBAB, A.—DESHAYES, F.: The T23/T24 Book, Vallourec & Mannesmann Tubes 2000.

[9] Vallourec & Mannesmann Tubes. Böhler Welding Group. Rohrstähle für Moderne Hochleistungskraftwerke. Sonderdruck aus "3R international", Heft 7, 2008.

[10] BENDICK, W.—GABREL, J.—HAHN, B.—VANDENBERGHE, B.: International Journal of Pressure Vessels and Piping, *84*, 2007, p. 13.

[11] BHADESHIA, H. K. D. H.: Lecture 10: Overall Transformation Kinetics II. Course MP6, Kinetics and Microstructure Modelling. Materials Science & Metallurgy Master of Philosophy, Materials Modelling. Cambridge University 2003.